

## ORIGINAL ARTICLE

# *HOXA1* drives melanoma tumor growth and metastasis and elicits an invasion gene expression signature that prognosticates clinical outcome

J Wardwell-Ozgo<sup>1</sup>, T Dogruluk<sup>1</sup>, A Gifford<sup>1</sup>, Y Zhang<sup>2</sup>, TP Heffernan<sup>3</sup>, R van Doorn<sup>4</sup>, CJ Creighton<sup>2</sup>, L Chin<sup>3,5,6</sup> and KL Scott<sup>1,2,6</sup>

Melanoma is a highly lethal malignancy notorious for its aggressive clinical course and eventual resistance to existing therapies. Currently, we possess a limited understanding of the genetic events driving melanoma progression, and much effort is focused on identifying pro-metastatic aberrations or perturbed signaling networks that constitute new therapeutic targets. In this study, we validate and assess the mechanism by which homeobox transcription factor A1 (*HOXA1*), a pro-invasion oncogene previously identified in a metastasis screen by our group, contributes to melanoma progression. Transcriptome and pathway profiling analyses of cells expressing *HOXA1* reveals upregulation of factors involved in diverse cytokine pathways that include the transforming growth factor beta (TGF $\beta$ ) signaling axis, which we further demonstrate to be required for *HOXA1*-mediated cell invasion in melanoma cells. Transcriptome profiling also shows *HOXA1*'s ability to potentially downregulate expression of microphthalmia-associated transcription factor (*MITF*) and other genes required for melanocyte differentiation, suggesting a mechanism by which *HOXA1* expression de-differentiates cells into a pro-invasive cell state concomitant with TGF $\beta$  activation. Our analysis of publicly available data sets indicate that the *HOXA1*-induced gene signature successfully categorizes melanoma specimens based on their metastatic potential and, importantly, is capable of stratifying melanoma patient risk for metastasis based on expression in primary tumors. Together, these validation data and mechanistic insights suggest that patients whose primary tumors express *HOXA1* are among a high-risk metastasis subgroup that should be considered for anti-TGF $\beta$  therapy in adjuvant settings. Moreover, further analysis of *HOXA1* target genes in melanoma may reveal new pathways or targets amenable to therapeutic intervention.

*Oncogene* (2014) 33, 1017–1026; doi:10.1038/onc.2013.30; published online 25 February 2013

**Keywords:** *HOXA1*; melanoma; metastasis; *MITF*; TGF $\beta$

## INTRODUCTION

Metastasis is responsible for greater than 90% of cancer-related deaths<sup>1</sup> and is primarily thought to occur through a complex progression of interrelated steps by which primary tumor cells acquire the capacity to invade adjacent tissue, enter and survive in circulation, extravasate and proliferate at distant organs sites.<sup>2</sup> This multifaceted process requires that cells acquire a wide range of biological capabilities to overcome numerous barriers to dissemination and growth in foreign microenvironments.

While much evidence supports this multi-step transit to metastasis, other data indicate that tumors may also be predestined with metastasis-promoting genetic events.<sup>3</sup> This deterministic model is supported by the finding that gene expression data derived from primary tumors can often predict metastasis<sup>4</sup> in addition to the fact that alterations found in metastases can be traced back to their subclonal presence in early primary lesions.<sup>5</sup> There is a great need to identify such early metastasis-promoting events or their activated pathways, particularly those with potential to serve as new therapeutic targets. Moreover, it is equally as important to continue efforts toward developing early cancer detection strategies and

intratumoral biomarkers that predict metastatic risk. This is especially true for aggressive cancers such as melanoma, whose current staging system is based on a measure of the vertical tumor thickness<sup>6</sup> in addition to other factors that include mitotic index, lymph node involvement and skin ulceration. Patients diagnosed with metastatic melanoma have an abysmal median survival of 6–9 months and a survival rate of only 10–20% due to melanoma's aggressive behavior and eventual resistance to all therapies.<sup>7</sup> Patients diagnosed with thin (<1 mm) melanoma have a high survival rate following tumor excision, and the majority of these individuals will have no evidence of metastasis at diagnosis. However, ~5–10% of melanoma patients with low-staged lesions (that is, Stage I/II) will die of recurrence and metastatic disease within 10 years of diagnosis despite surgical removal of the primary tumor.<sup>8</sup> This is further evidenced by a retrospective study of 9129 fatal melanoma cases spanning 1988–2006 that discovered, among patients developing lethal metastatic disease, an equivalent number had been diagnosed with thin (<1 mm; 2472 cases) as with thick (>4 mm; 2041 cases) melanomas.<sup>9</sup> These statistics suggest that there is a high-risk melanoma

<sup>1</sup>Department of Molecular and Human Genetics, Baylor College of Medicine, Houston, TX, USA; <sup>2</sup>Dan L. Duncan Cancer Center, Baylor College of Medicine, Houston, TX, USA;

<sup>3</sup>Institute for Applied Cancer Science, University of Texas M.D. Anderson Cancer Center, Houston, TX, USA; <sup>4</sup>Department of Dermatology; Leiden University Medical Center, Leiden, The Netherlands and <sup>5</sup>Department of Genomic Medicine, Houston, TX, USA. Correspondence: Dr KL Scott, Department of Molecular and Human Genetics, Baylor College of Medicine, One Baylor Plaza, BCM225, Houston, TX 77030, USA.

E-mail: kls1@bcm.edu

<sup>6</sup>These authors contributed equally to this work.

Received 16 May 2012; revised 5 December 2012; accepted 27 December 2012; published online 25 February 2013

sub-population that is not identified by the current standard pathological and clinical staging system and illustrate the need for new molecular-based risk assessment strategies and novel targeted therapeutics to manage this aggressive malignant disease.

Given the pressing need to identify genetic mediators of melanoma metastasis and better prognostic indicators, we devised an oncogenomics-guided screening strategy to identify genes capable of driving cancer cell invasion and metastasis.<sup>10</sup> This approach leveraged a multi-level oncogenomics comparison founded on (1) genetically engineered mouse models of melanoma with differing metastatic potential and (2) genomics data derived from human melanoma. These methods revealed a conserved list of 360 genes correlating with metastatic potential, functional screening of which identified 18 genes whose ectopic expression could significantly enhance cell invasion. Among those 18 genes, our initial study focused on validating the *ACP5* phosphatase, expression of which we found to not only enhance melanoma cell invasion but also drive *in vivo* tumorigenesis and metastasis by a mechanism involving modulation of the phosphorylation status of proteins comprising the focal adhesion complex.

In this study, we validate the top performing pro-invasion candidate identified by our initial screening approach, homeobox transcription factor A1 (*HOXA1*). We demonstrate that *HOXA1* exhibits pro-invasive and oncogenic activities across several melanoma cell systems in a manner dependent on *HOXA1*'s functional DNA binding domain. Transcriptome profiling comparisons reveal *HOXA1*'s marked influence on the expression of genes involved in diverse cytokine signaling pathways, and cell-based studies support a mechanism by which *HOXA1* hyperactivates the transforming growth factor beta (TGF $\beta$ ) signaling pathway to elicit *HOXA1*-mediated cell invasion. Finally, we provide evidence that *HOXA1* potentially downregulates genes involved in melanocyte differentiation, suggesting that *HOXA1* expression de-differentiates cells into a state with higher metastatic potential. Importantly, the *HOXA1* gene signature successfully stratifies melanoma patients into two subgroups with significant differences in metastasis-free survival based on expression in primary tumor specimens, suggesting that this prognostic signature may provide insight into new means by which to identify at risk patients and potentially reveal new targets for therapeutic intervention.

## RESULTS

Functional validation of *HOXA1* as a pro-invasion oncogene in melanoma

In a recent effort to identify early genetic drivers of melanoma metastasis,<sup>10</sup> we devised a comparative oncogenomics strategy employing use of genomics data derived from human and genetically engineered mouse melanoma tumors originating from: (1) an inducible *H-RAS*<sup>G12V</sup>-driven model (iHRAS) that develops non-metastatic tumors<sup>11</sup> and (2) a similarly engineered model for induction of the receptor tyrosine kinase *MET* (iMET) that initiates metastatic melanomas.<sup>10</sup> Gene candidates identified by this *in silico* strategy were enlisted into a functional screen for drivers of *in vitro* cell invasion, an effort that identified *HOXA1* as the top-scoring pro-invasion gene.<sup>10</sup> To begin our validation efforts on *HOXA1* in this study, we sought to examine *HOXA1* activity in *Ink4a/Arf*<sup>-/-</sup> mouse-derived melanocytes transduced with *H-RAS*<sup>G12V</sup> (hereafter referred to as M3HRAS cells<sup>12</sup>) given that our candidate gene list was derived from genomic comparisons of non-metastatic iHRAS and metastatic iMet genetically engineered mouse tumors. Non-metastatic M3HRAS cells stably expressing *HOXA1* exhibited increased invasion through Matrigel by 12-fold compared with vector control cells in transwell invasion assays (Figure 1a;  $P=0.0185$ ). Even more striking was *HOXA1*'s ability to enhance macroscopic lung nodule formation by M3HRAS cells

following intravenous injection into NOD-SCID mouse tail veins, a surrogate assay for metastasis (Figure 1b). Consistent with these pro-invasion and metastatic phenotypes, expression of *HOXA1* in M3HRAS cells induced an invasive cell morphology characterized by invasive, stellate protrusions when plated in Matrigel matrix compared with M3HRAS vector control cells that proliferated as individual colonies devoid of invasive structures (Figure 1c). Together, these data demonstrate the pro-invasive activity of *HOXA1* in an M3HRAS cells thereby supporting its role of as a pro-metastasis gene identified from our initial comparison of iHRAS and iMet tumors.

Given *HOXA1*'s robust activities in the murine M3HRAS cell line, we sought to validate *HOXA1*'s activity in human melanoma cell line models. As demonstrated previously,<sup>10</sup> expressing *HOXA1* in engineered TERT immortalized melanocytes expressing *BRAF*<sup>V600E</sup> (*PMEL/hTERT/CDK4(R24C)/p53DD*)<sup>13</sup> hereafter referred to as 'HME468') enhanced *in vitro* cell invasion ~10-fold over vector-expressing control cells (Figure 1d;  $P<0.0001$ ). Likewise, *HOXA1* greatly enhanced cell invasion over vector control cells when expressed in weakly invasive cell lines that include WM115 (Figure 1d;  $P=0.0024$ ) and to a lesser extent in WM3211 cells (Figure 1d;  $P=0.0172$ ). The phenotypic effect of expressing *HOXA1* appeared most dramatic on WM115, as cells transduced with *HOXA1* underwent a dramatic change in morphology (Figure 1e) denoted by a marked increase in cell spreading, membrane ruffling (Supplementary Movies S1 and S2), and invasive protrusions when plated in Matrigel matrix (Figure 1f) with no obvious changes in cell proliferation (Supplementary Figure S1) compared with vector-expressing control cells.

We showed previously that *HOXA1* displays a pattern of progression-correlated expression across the benign-to-malignant transition, exhibits oncogenic activity when expressed with *BRAF*<sup>V600E</sup> in immortalized melanocytes and is required to maintain anchorage-independent growth.<sup>10</sup> Given *HOXA1*'s pronounced phenotypic effects on the weakly tumorigenic WM115 melanoma cell line (Figures 1d–f), we next examined *HOXA1*'s ability to enhance WM115 colony formation in anchorage-independent growth assays. As expected, expressing *HOXA1* markedly enhanced WM115 colony formation 10.6-fold compared with vector-expressing cells when plated in soft agar assays (Figure 2a;  $P<0.0001$ ). Consistent with this *in vitro* study, we next examined *HOXA1*'s ability to enhance tumor growth by implanting WM115 cells expressing *HOXA1* or vector control into the flanks of athymic mice. *HOXA1* expression led to a significant increase in xenograft tumor incidence ( $P=0.0051$ ) and growth ( $P<0.0001$ ) compared with control cells that largely failed to form palpable tumors within the time course of these studies (Figure 2b). To confirm this finding, we constructed a WM115 cell line with a doxycycline inducible *HOXA1* expression construct, whose activation with doxycycline following cell implantation led to an increase in tumor growth compared with a control mouse cohort maintained off of doxycycline (Figure 2c;  $P=0.0057$ ). These validation data support a pro-tumorigenic role for *HOXA1* in melanoma and together with the progression correlation data and our previous finding that *HOXA1* can cooperatively transform immortalized primary melanocytes expressing *BRAF*<sup>V600D</sup>,<sup>10</sup> suggests that *HOXA1* may be selected for early during transformation where it also drives tumor metastasis.

To begin investigating the mechanism by which *HOXA1* influences cell invasion and tumor growth, we mutated homeodomain residues glutamine 50 and asparagine 51 to alanine (QN > AA) which has been shown by others to impair DNA binding activity of *HOXA1*.<sup>14</sup> In contrast to WM115 cells expressing wild-type *HOXA1*, cells stably expressing the homeodomain dead (HD) mutant failed to increase cell invasion compared with WM115 control cells despite being expressed at similar levels (Figure 2d). Similarly, WM115 cells expressing *HOXA1*-HD failed to recapitulate *HOXA1*-mediated increases in *in vivo* tumor growth following

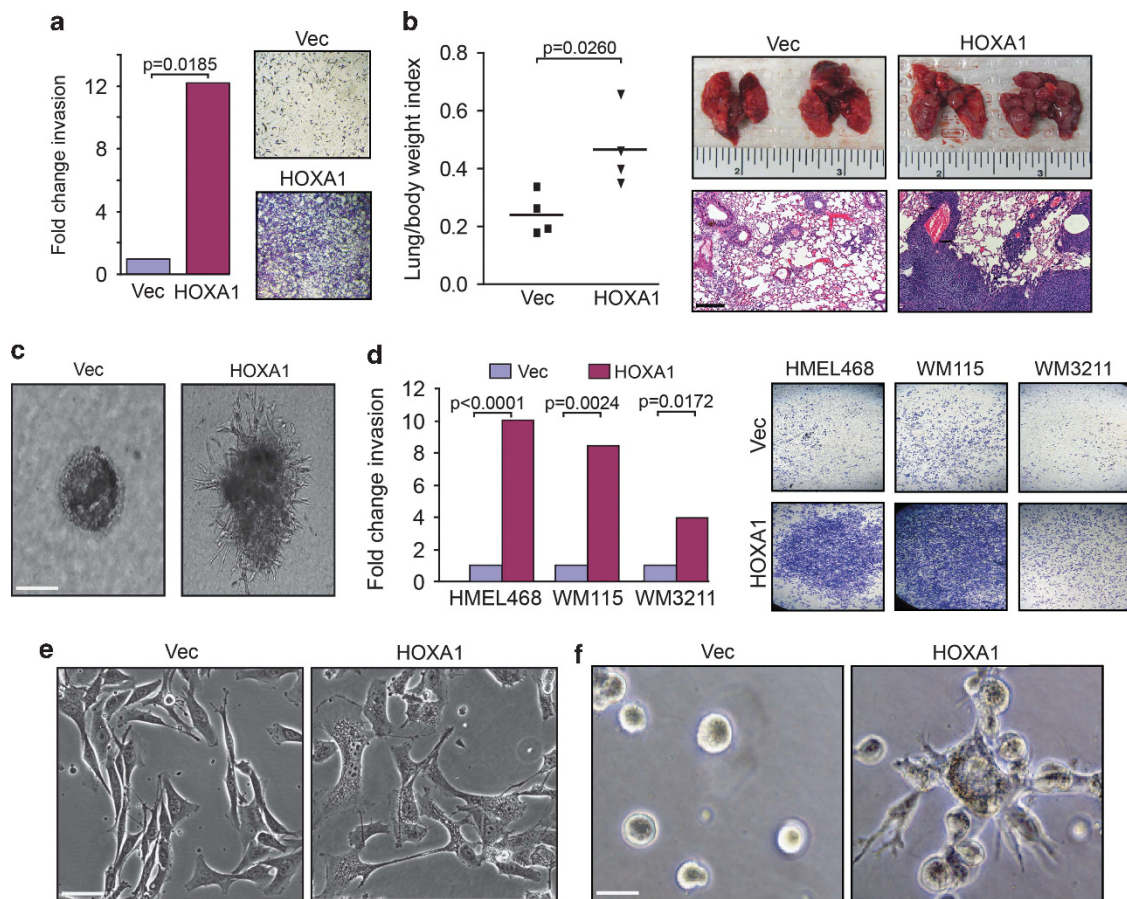


**Figure 1.** HOXA1 drives cell invasion and metastasis in weakly metastatic melanoma models. (a–c) M3HRAS cells overexpressing vector control (Vec) or *HOXA1* were assayed for (a) *in vitro* invasion using transwell Matrigel invasion chambers (b) lung seeding capacity, a correlate of metastatic activity, following intravenous injection into mouse tail veins and (c) invasive morphology in 3D Matrigel colony assays. Images in (a) show representative invasion readouts and (b) H&E stained lung sections harvested from experimental animals. *P*-values calculated by *t*-test. Scale bars = 100 μm (b); 50 μm (c). (d) Human cell lines HME468, WM115 and WM3211 overexpressing vector control or *HOXA1* were assayed for *in vitro* invasion using transwell invasion chambers. Representative invasion readouts shown at right. *P*-value calculated by *t*-test. (e, f) WM115 cells expressing vector control or *HOXA1* propagated in (e) 2D tissue culture and (f) 3D Matrigel colony formation assays. Scale bars = 100 μm (e); 50 μm (f).

implantation into athymic mice (Figure 2e). Mutating the DNA binding domain completely abolished *HOXA1*'s ability to promote anchorage-independent growth in soft agar (Figure 2f; wild type versus HD,  $P < 0.0001$ ), and comparison of vector- and *HOXA1*-HD-expressing cells suggests that *HOXA1*-HD exhibits a dominant-negative effect in this assay ( $P = 0.0068$ ). Together, these data suggest that *HOXA1* requires its native ability to bind DNA to elicit invasive and oncogenic effects, likely due to its transcription factor activity.

#### Transcriptome analysis links *HOXA1* to cytokine signaling pathways

Our finding that *HOXA1* requires its native ability to bind DNA to elicit its pro-invasion and oncogenic activities combined with its known role as a transcription factor led us to examine the *HOXA1* transcriptome to gain insight into the protein's mode-of-action in melanoma. Given the strong phenotypes exhibited by WM115 cells following enforced expression of *HOXA1*, we chose to first profile WM115 cells stably expressing *HOXA1* or vector control using Affymetrix gene chips. Analysis for differential gene expression revealed 852 upregulated and 882 downregulated genes ( $P < 0.01$ , >3-fold change, average intensity >25) in cells constitutively expressing *HOXA1* (Supplementary Table S1), which

is consistent with *HOX* genes' ability to both activate and repress gene transcription.<sup>15</sup> Functional annotation clustering via David Bioinformatics Resources revealed 'regulation of cell migration' ( $P = 5.67E - 10$ ) as the top-scoring functional group (Supplementary Table S2). A large portion of the differentially expressed genes (249 upregulated and 192 downregulated) exhibited a greater than 10-fold change in expression in WM115-*HOXA1* cells compared with vector control cells (Supplementary Table S1). Closer analysis of the upregulated gene set (>10-fold change) indicated significant enrichment for 'secreted factors' ( $P = 5.5E - 26$ ), 'extracellular region' ( $P = 7.7E - 19$ ), 'chemotaxis' ( $P = 3.2E - 10$ ) and 'cytokine activity' ( $P = 2.7E - 09$ ) among the top functional groups (Supplementary Table S2). Knowledge-based pathway analysis using IPA revealed a top-scoring network (Supplementary Figure S2) whose node centered on TGFβ1, a cytokine that regulates diverse cellular processes that include cell growth, movement, differentiation and apoptosis.<sup>16</sup>

Given the known role for the TGFβ pathway in regulating cancer progression processes, we used WM115 cells to perform a focused PCR profiling array to analyze *HOXA1*-induced expression changes of 84 genes associated with the TGFβ/bone morphogenic protein (BMP) signaling pathway. These assays confirmed that expression of *HOXA1* significantly modulates expression of multiple genes encoding components that signal through this pathway that



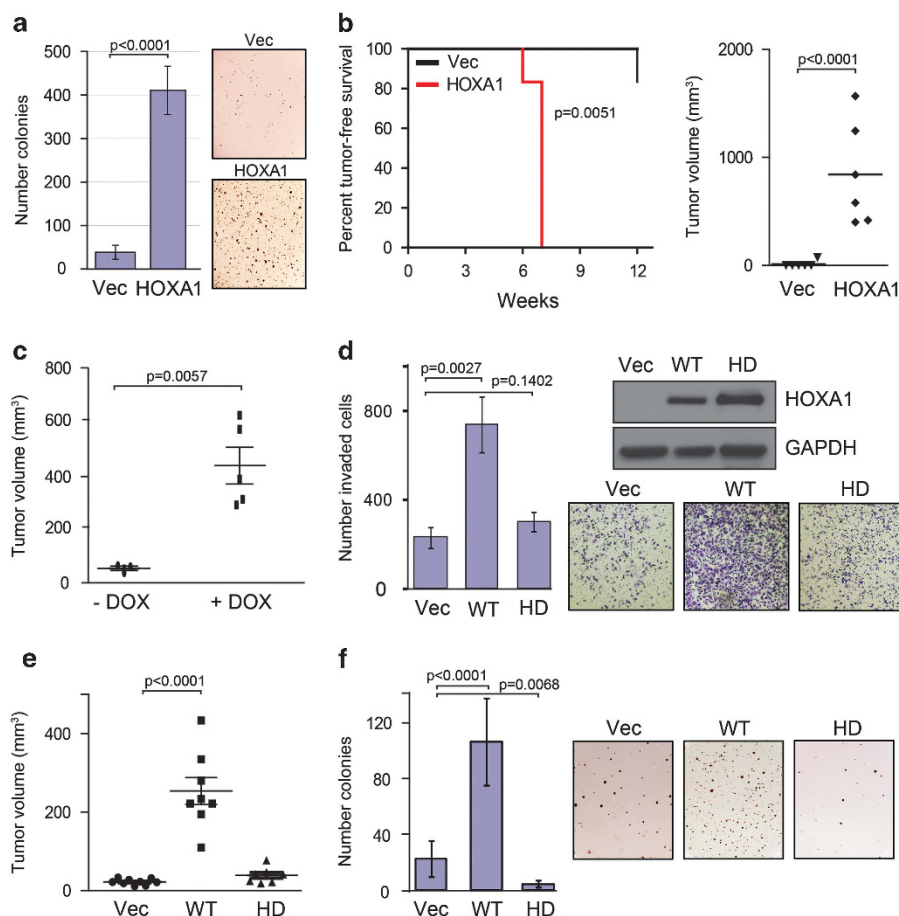


**Figure 2.** *HOXA1*-mediated oncogenicity requires a functional DNA binding domain. (a, b) WM115 cells expressing vector control (Vec) or *HOXA1* were assessed for (a) colony formation in anchorage-independent growth assays and (b) xenograft tumor growth in athymic mice. Kaplan–Meier tumor-free survival (left) and endpoint tumor size (right) are shown for (b). (c) End point size analysis of WM115 xenograft tumors induced by a doxycycline (DOX)-inducible *HOXA1* construct. (d–f) WM115 cells stably expressing vector control (Vec), *HOXA1* (wild type (WT)) or *HOXA1* mutated at its DNA binding domain (HD) were examined for (d) *in vitro* invasion activity using transwell invasion chambers, (e) xenograft tumor growth and (f) anchorage-independent growth. The immunoblot shown in (d) reflects the level of WT *HOXA1* and *HOXA1*-HD protein expressed in cells used for experiments shown in (d–f). Error bars indicated  $\pm$  s.d.; all *P*-values calculated by *t*-test except for Figure 1b, left (*P*-value calculated by log rank).

include receptors (for example, *PDGFB*,  $9.5 \times$ ; *BMPR1B*,  $-126.7 \times$ ), ligands (for example, *BMP7*,  $9.5 \times$ ; *TGFB1*,  $5.9 \times$ ; *GDF5*,  $6.7 \times$ ) and other molecules (for example, *SERPINE1/PAI-1*,  $18.8 \times$ , *CER1*,  $-4.7 \times$ ) positioned throughout the TGF $\beta$  signaling axis (Figure 3a). As a more directed measure of *HOXA1*'s influence on TGF $\beta$  signaling, we transfected control and *HOXA1*-expressing WM115 cells with a TGF $\beta$ -responsive reporter construct (p3TP-Lux;<sup>17</sup>). As shown in Figure 3b, expression of *HOXA1* enhanced basal reporter activity (11.0-fold,  $P = 0.0030$ ) in the absence of TGF $\beta$  and evoked a 9.3-fold increase in response to TGF $\beta$  ligand compared with control cells ( $P < 0.0001$ ). Correspondingly, levels of phosphorylated SMAD3 (p-SMAD3), which is the activated form of this protein and is required for signaling through the TGF $\beta$  pathway, were elevated in cells expressing *HOXA1* and increased further after stimulation with TGF $\beta$  ligand thus corroborating active TGF $\beta$  signaling (Figure 3c). Notably, total SMAD3 levels were also elevated in *HOXA1*-expressing cells (Figure 3c), which is consistent with SMAD3's fourfold upregulation observed from our transcriptome analysis (Supplementary Table S1). To determine whether *HOXA1*-mediated invasion is dependent on the TGF $\beta$  pathway, we treated control- and *HOXA1*-expressing cells with RNAi against SMAD3. Depletion of SMAD3 decreased *HOXA1*-mediated invasion (Figure 3d), which further

indicates that *HOXA1* requires the TGF $\beta$  pathway to fully elicit its pro-invasion phenotype.

#### HOXA1 regulates expression genes controlling melanocyte differentiation

In contrast to the *HOXA1*-induced upregulated genes, functional clustering analysis of genes downregulated by *HOXA1* greater than 10-fold revealed groups related to melanocyte biology, particularly 'pigmentation during development' ( $P = 1.9E - 05$ ) and 'melanocyte differentiation' ( $P = 8.0E - 05$ ) (Supplementary Table S2). In support of this finding, knowledge-based pathway analysis using IPA revealed a top-scoring downregulated network whose node centered on microphthalmia-associated transcription factor (*MITF*; average 28-fold downregulation in *HOXA1*-expressing cells), a transcription factor critically important for activating expression of genes required for melanocyte differentiation from their neural crest precursors (Figure 4a, box). Immunoblotting analysis of WM115 protein lysates confirmed decreased *MITF* protein expression in cells expressing *HOXA1* versus vector control (Figure 4b).

In addition to *MITF*, we identified components of the *MITF* signaling network including multiple *MITF* target genes that

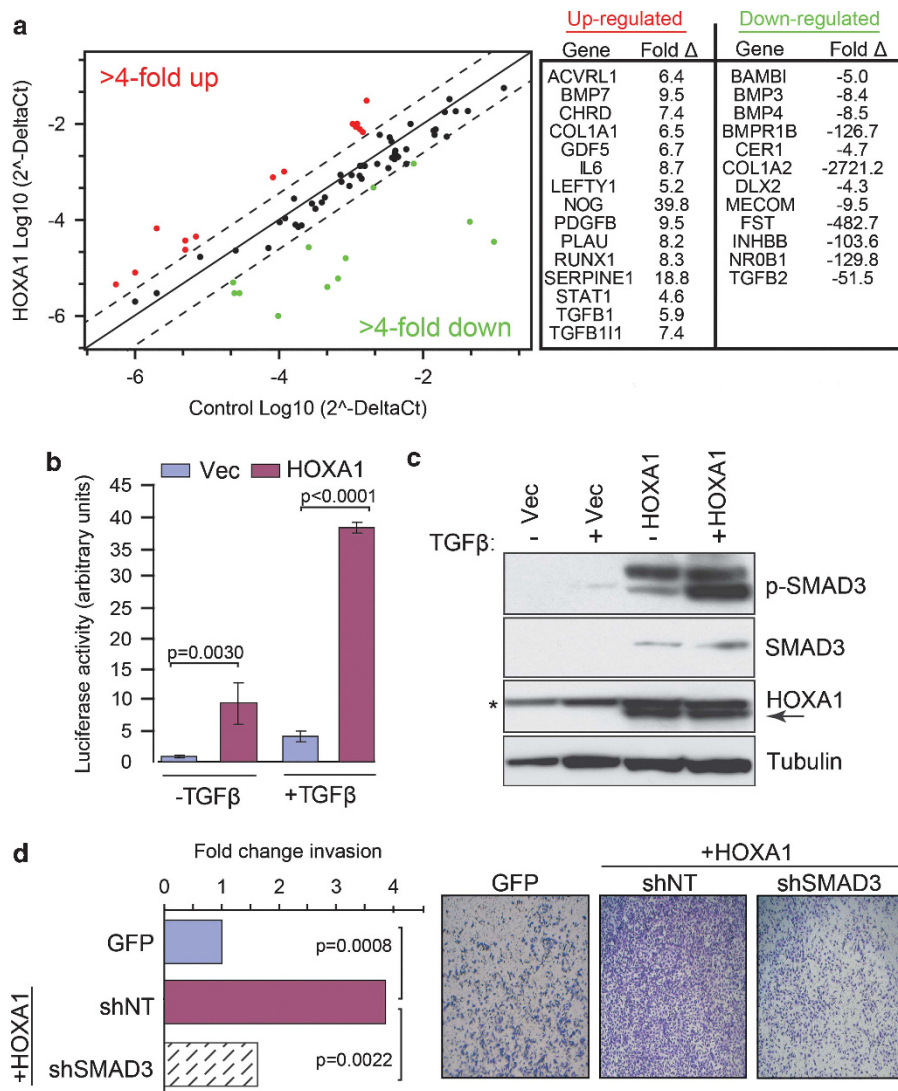


**Figure 3.** *HOXA1* promotes invasion through enhanced TGFβ signaling. (a) Focused TGFβ/BMP PCR profiling array on cDNA isolated from WM115 cells stably expressing vector control or *HOXA1*. Genes upregulated (red) and downregulated (green) greater than fourfold in *HOXA1*-expressing cells compared with vector control are shown at right. (b) WM115 cells expressing vector control (Vec) or *HOXA1* were transfected with the TGFβ-inducible p3TP-Lux luciferase reporter construct, followed by treatment with or without TGFβ to assess responsiveness. Error bars indicate  $\pm$  s.d.; *P*-values calculated by *t*-test. (c) Whole cell lysates from WM115 cells stably expressing vector control or *HOXA1* were propagated in 1% serum with or without TGFβ for immunoblot analysis using the indicated antibodies. *P*-SMAD3 = phosphorylated SMAD3, Ser423 + Ser425. \*Denotes tubulin band. (d) WM115 cells expressing vector control or *HOXA1* were treated with or without *SMAD3* shRNA (shSMAD3) or non-targeting shRNA (shNT) and loaded onto transwell invasion chambers. *P*-values calculated by *t*-test.

include *DCT* ( $-177.3 \times$ ), *TYRP1* ( $-23.1 \times$ ) and *GPNNB* ( $-22.7 \times$ ) among others based on their probe set expression averages (Figure 4c), and additional *MITF* targets that were present in our transcriptome analysis but not included in the IPA-generated network including *EDNRB* ( $-90.8 \times$ ), *TYR* ( $-6 \times$ ) and *TBX2* ( $-5.1 \times$ ) (Supplementary Table S1). Quantitative PCR analysis of mRNA isolated from WM115 cells expressing *HOXA1* or vector control validated differential expression of select *MITF* target genes and others found overexpressed in our transcriptome analysis (Figure 4d), providing additional evidence to support the regulation of these candidates by *HOXA1*. Importantly, we detected the same trend in upregulated and downregulated expression of this target gene set in two WM115 tumors (396 and 397) resulting from our *in vivo* explant studies (Figure 2c) that employed the doxycycline-inducible *HOXA1* system (Supplementary Figure S3). We extended this analysis to three additional melanoma cell lines with documented *MITF* expression

(Supplementary Figure S4). Expression of *HOXA1* in SkMel30 cells (high *MITF*) resulted in a trend of panel gene expression similar to observed with WM115 cells and tumors, whereas *HOXA1* was less effective at evoking this response in low *MITF*-expressing cell lines WM278 and CHL-1 (Figure 4d).

Consistent with this latter finding was our observation that *HOXA1* failed to increase cell invasion when expressed in the WM278 and CHL-1 cell lines (Supplementary Figure S5) and exhibited weak pro-invasion activity when expressed in the low *MITF*-expressing WM3211 cell line compared with the high *MITF*-expressing cell lines, HME468 and WM115 (Figure 1d). Moreover, expressing *HOXA1* in SkMel30 cells (high *MITF*) significantly reduced *MITF* at the protein level similar to observed in WM115 cells (Figure 4b). Use of a previously described<sup>18</sup> signature scoring metric ('*t*-score') to compare the WM115 transcriptome data sets with transcriptome data derived from SkMel30 cells expressing vector control or *HOXA1* (Supplementary Table S1) revealed a high

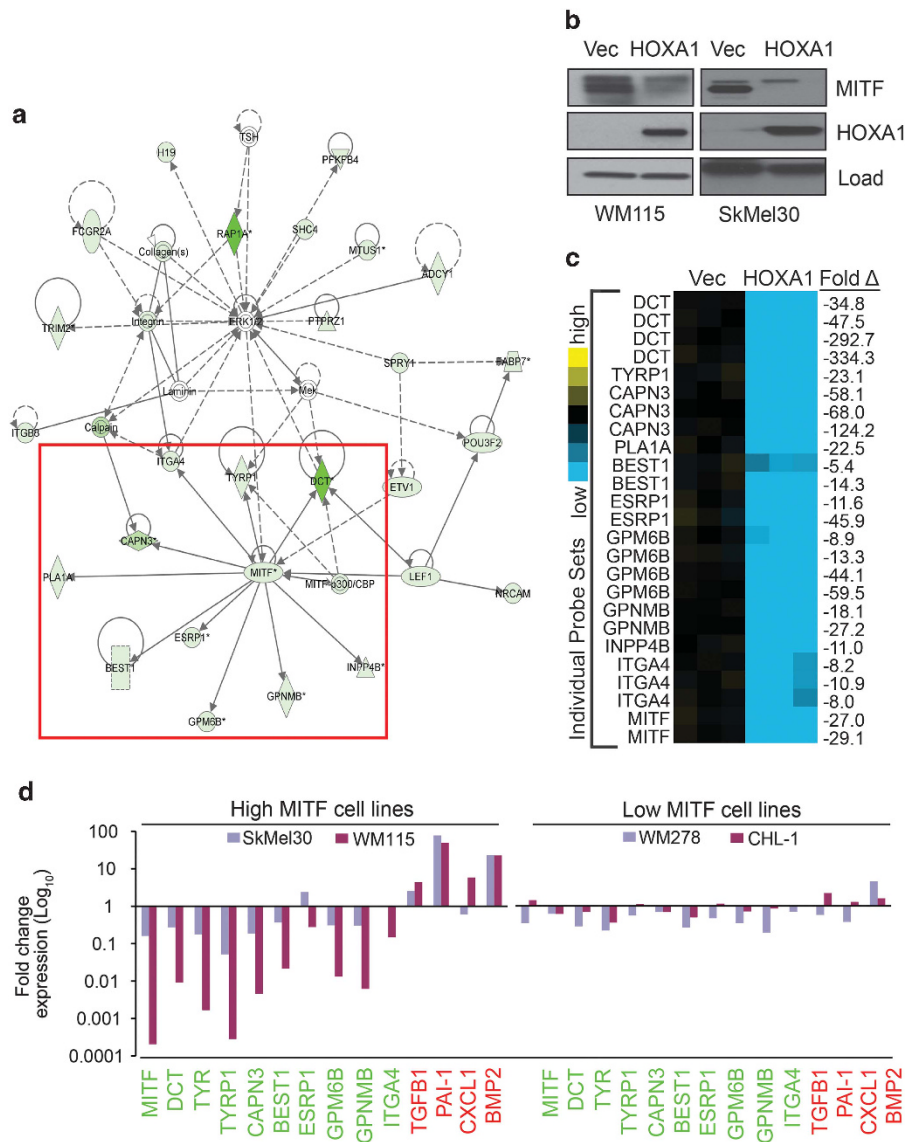


**Figure 4.** *HOXA1* expression downregulates genes important for melanocyte differentiation and pigmentation. **(a)** Molecule network generated using IPA. The network is displayed graphically as nodes (genes) and edges (the biological relationships between nodes). Solid lines represent direct interactions and dashed lines represent indirect interactions. Green colors denote genes that were underexpressed > 10-fold in WM115 expressing *HOXA1* versus control. Red box surrounds *MITF* node and known *MITF* target genes differentially expressed > 10-fold in WM115-*HOXA1* cells. **(b)** Whole cell lysates from WM115 and SkMel30 cells stably expressing vector control (Vec) or *HOXA1* were processed for immunoblot analysis using the indicated antibodies. Load = tubulin (WM115 panel) and GAPDH (SkMel30 panel). **(c)** Heat map representing Affymetrix probe expression for genes boxed in **(a)**. Expression values at right indicate fold change in gene expression (*HOXA1* versus vector control). **(d)** Expression validation of select genes by RT-qPCR analysis of cDNA prepared from WM115 and SkMel30 (high MITF) and WM278 and CHL-1 (low MITF) cells expressing vector control or *HOXA1*. All values are normalized based on Actin B expression and plotted as fold change compared with vector control (set as 1.0 for each gene). Values indicate fold change for genes found upregulated (red) and downregulated (green) in WM115 transcriptome analysis.

degree of similarity between the signatures (Supplementary Figure S6). In contrast, *T*-score analysis indicated a low degree similarity when comparing the WM115- and WM3211 (low MITF)-derived signatures (Supplementary Figure S6). Together, these data suggest that *HOXA1* expression drives deregulation of melanocytic development genes, and *HOXA1*'s phenotypic effects are greatest when expressed in parental cells with high levels of MITF.

*HOXA1* promotes an invasive gene signature and prognosticates clinical outcome

*HOXA1*'s potent effects on cell invasion led us to explore published transcriptome profiling studies that have produced melanoma

invasion gene signatures. One such study by Hoek *et al.*<sup>19</sup> reported an expression clustering analysis that differentiated 86 melanoma specimens from three sample cohorts (Zürich, Philadelphia and Mannheim data sets; GEO accession GSE4845) into three distinct cluster groups (A–C) based on related transcriptome profiles. Comparing our *HOXA1*-induced expression signature with those of group A (weakly invasive), group B (intermediate) and group C (highly invasive) using the *t*-score metric indicated a significant degree of similarity with group C in each of the Zürich, Philadelphia and Mannheim cohorts (Figure 5a; *t*-test for *t*-score values: A and B versus C,  $P = 4.8E - 08$ ). Based on the authors' functional annotation of the genes differentiating groups A–C,<sup>19</sup> the genes in the invasive group C differ from those of weakly



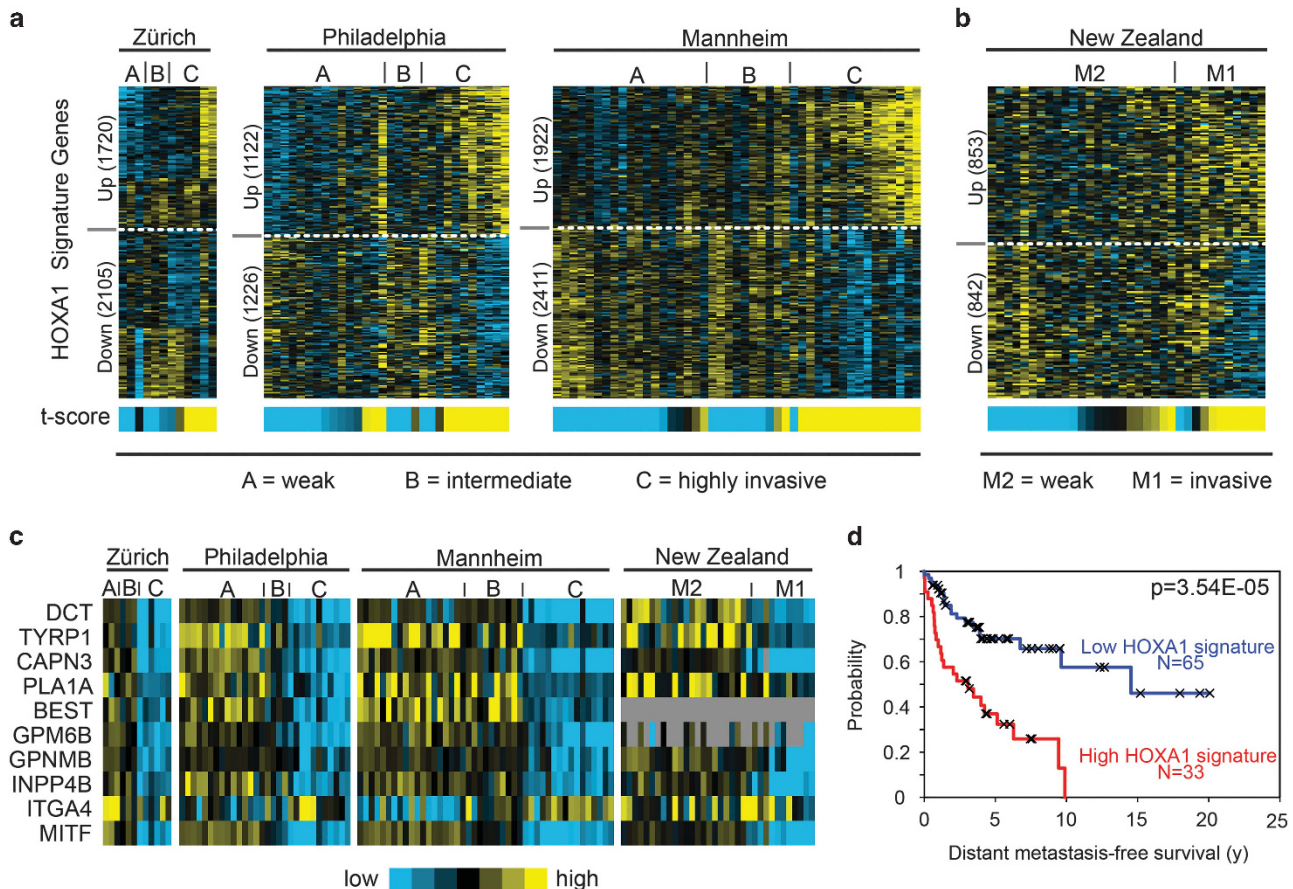


**Figure 5.** *HOXA1* expression signature correlates with invasiveness and prognosticates patient clinical outcome. **(a, b)** Heat map representing expression of *HOXA1* signature genes in transcriptome profiles of melanoma specimens collected by **(a)** Hoek *et al.*<sup>19</sup> (N: Zürich, 15; Philadelphia, 55; Mannheim, 45) and **(b)** Jeffs *et al.*<sup>20</sup> (N: 34). Specimens in **(a)** are annotated based on the presence or absence of invasive gene signature defined in Hoek *et al.*<sup>19</sup>: A = weakly invasive, B = intermediate, C = highly invasive, whereas specimens in **(b)** are annotated based on the presence or absence of motifs defined in Jeffs *et al.*<sup>20</sup>: M1 = invasive, M2 = weakly invasive. Signature similarity score (t-score) is represented by heat map bar (blue, low; yellow, high). **(c)** Heat map representing expression of *MITF* and select *MITF* target genes (see Figures 4c and d) in the transcriptome reported by Hoek *et al.*<sup>19</sup> and Jeffs *et al.*<sup>20</sup> **(d)** Differences in patient outcome based on *HOXA1* gene signature manifestation (comparing samples in the top 25% of signature scores with those in the bottom 75%) using a cohort of 98 primary melanomas reported by Winnepenninckx *et al.*<sup>22</sup>; P-value calculated by log-rank test.

invasive group A based on the presence of 51 downregulated genes that are enriched for neural crest and melanocytic differentiation factors and 54 upregulated genes enriched for extracellular modifying factors and genes regulated by TGF $\beta$  signaling. Of these 105 genes, the *HOXA1*-induced gene signature contained 31 of 51 downregulated genes that included *MITF*, *TYRP1*, *TYR* and *DCT* among others. In addition, our *HOXA1*-induced gene signature contained 29 of 54 genes significantly upregulated in the group C transcriptome.

In addition to studies by Hoek *et al.*, we similarly examined expression data recently reported by Jeffs *et al.*<sup>20</sup> who profiled a large cohort of cell lines derived from primary melanomas (New Zealand data set; GEO accession GSE16404). Like the previous study, Jeffs *et al.* employed unsupervised clustering analysis that defined two motifs of cell lines based on expression of a core set of genes that included *MITF* and others involved in such processes as neural crest development, melanocytic differentiation and extracellular matrix remodeling. Comparing the *HOXA1* signature with the Jeffs *et al.* data set indicated a degree of similarity with expression Motif 1, which is characterized by low *MITF* and high invasion activity, versus expression Motif 2 that contains higher *MITF* levels, downregulation of extracellular remodeling factors and are weakly invasive (Figure 5b; t-test for t-score values: Motif 1

versus Motif 2,  $P=0.0003$ ). Similarly to invasive group C specimens defined by Hoek *et al.*<sup>19</sup> cell lines characterized by the invasive Motif 1 were enriched for *MITF* target genes which are also downregulated by *HOXA1* expression >10-fold (Figure 5c) and residing in the *MITF* network illustrated in Figure 4a. Together, these data suggest that enforced expression of *HOXA1* drives cells to adopt an invasion profile through a process reminiscent of de-differentiation into a neural crest-like cell type with higher metastatic potential.

These findings led us to explore the prognostic implications of the *HOXA1* gene signature in melanoma. Given the shortage of outcome-associated expression data sets for melanoma, which is primarily due to limited availability of primary human melanoma tissue preserved in a form suitable for expression profiling,<sup>21</sup> we focused on a data set<sup>22</sup> containing a cohort of 98 primary tumor specimens (combined study and validation sets: Stage I, II, III and IV tumors) with accompanying patient outcome data. We scored these profiles for similarity to the *HOXA1* gene signature and found that patients with profiles showing more similarity to the *HOXA1*-inducible patterns had a shorter time to distant metastasis events (univariate Cox  $P<0.01$ , t-score as continuous variable; log-rank test  $P=3.5E-05$ , comparing top 25% of high scoring samples versus others, Figure 5d). Multivariate Cox analysis

incorporating established clinical variables (stage, age and tumor thickness) indicate that the *HOXA1* gene signature provides additional prognostic power independent of these main clinical variables (Supplementary Table S3). Together, these data indicate that the *HOXA1* gene signature prognosticates patient risk based on expression in primary tumors.

## DISCUSSION

The purpose of this study was to functionally validate and elucidate the mechanism-of-action for *HOXA1*, the top-scoring pro-invasion gene identified from our recently described oncogenomics-guided screen for melanoma metastasis drivers.<sup>10</sup> *HOXA1* is a conserved member of the homeobox transcription factor family, which comprising 39 genes in humans organized into four different clusters (A–D) that coordinately regulate cell fate, early developmental patterns and organogenesis.<sup>23</sup> Complex transcription networks have evolved to spatially and temporally regulate *HOX* gene expression during development, and a growing body of evidence suggests that disrupting this tight regulation can impact oncogenic and tumor suppressive mechanisms in a context-specific manner.<sup>23</sup> Indeed, *HOX* genes have been found to directly impact tumorigenesis via diverse mechanisms in cancers that include lung, breast and hematological malignancies among others, and *HOXA1* upregulation has specifically been reported in cancers including breast cancer, leukemia, squamous cell carcinoma and melanoma, including in melanomas with distant metastasis.<sup>24</sup>

*HOXA1*'s role as a transcription factor coupled with our current findings that described *HOXA1*-mediated cancer activities require its functional DNA binding domain led us to examine gene expression changes elicited by *HOXA1* in melanoma cells. From those studies an invasive expression profile emerged that includes increased expression of numerous cytokines and their mediators, including those involved with TGF $\beta$ /BMP signaling. We demonstrate that *HOXA1* expression enhances activation of the TGF $\beta$  pathway, and we further show that the SMAD signaling axis required for TGF $\beta$ -mediated processes is required for *HOXA1* to elicit its full effects on *in vitro* cell invasion. While it remains unclear how *HOXA1* mediates TGF $\beta$  signaling and whether *HOXA1* also functions through other cytokine signaling pathways identified by our transcription analysis, it is intriguing to speculate that this pathway may be in some way connected to an altered cell differentiation program given the role played by *HOX* genes in cell fate determination. This notion is supported by our transcriptome analysis that revealed marked de-regulation of genes involved in melanocytic differentiation that included *MITF*, which is a melanocytic lineage-specific transcription factor that serves as a central regulator in melanocyte determination, as well as key *MITF* downstream targets. Other studies have provided a mechanism for oncogenesis by which some *HOX* genes re-express in tumors in a manner temporally different from expression in their parental, normal tissue to disrupt cell differentiation pathways.<sup>23</sup> It is interesting to note that mouse studies have shown that *HOXA1* expression is tightly regulated between days 7 and 9 of embryonic development where it is expressed in neural crest precursors essential for the generation of mesenchymal derivatives that include melanocytes among other cell lineages.<sup>25</sup> Future work will determine whether late, mis-expression of *HOXA1* promotes melanoma tumor growth and metastasis by a mechanism that may involve de-differentiating cells into a more mobile, invasive neural crest-like precursor state.

While additional studies are required to determine whether *HOXA1* directly regulates expression of melanocytic differentiation genes like *MITF*, it is noteworthy that decreased expression of *MITF* has previously been associated with increased melanoma invasiveness<sup>26</sup> whereas *MITF* overexpression has been demonstrated to suppress melanoma metastasis.<sup>27</sup> Hoek et al.<sup>28</sup> have similarly

documented a pattern of decreased *MITF* expression in invasive cell lines, an observation that led to the 'phenotype switching' hypothesis proposed to account for melanoma metastasis. In contrast to the stochastic view that pro-metastatic genomic alterations occur in a step-wise manner during tumor evolution, the phenotype switching hypothesis posits that genes required for metastasis are epigenetically modulated to change individual cells from a proliferative to a more invasive cell state.<sup>29</sup> It is tempting to speculate that *HOXA1* directly influences phenotype switching behavior given similarities between the *HOXA1*-induced gene signature and those reported by Hoek et al. It is unclear how *HOXA1* coordinately downregulates the melanocytic differentiation pathway and activates signaling through the TGF $\beta$  axis, though prior work has suggested that TGF $\beta$  represses *MITF* expression.<sup>30</sup> Moreover, other work<sup>31</sup> reported that mobile, metastatic melanoma cells express low levels of *MITF* and exhibited increased TGF $\beta$  activation compared with non-motile cells that expressed high levels of *MITF*. Given *HOXA1*'s profound effect on TGF $\beta$  signaling and suppression of *MITF* and its targets, it is possible that *HOXA1* could be a regulator of phenotype switching and suggests a model by which decreased expression of *MITF* and increased signaling through the TGF $\beta$  axis coordinately drive melanoma growth and metastasis.

Our finding that the *HOXA1* gene signature predicts clinical outcome based on expression profiles of primary tumors suggests that it might be useful to stratify metastatic risk for patients with melanoma, though more work will be required to validate its prognostic utility. Such a molecular prognostic test, if successfully implemented in the clinic, would significantly complement current prognostication standards by identifying high-risk sub-populations from generally low-risk, early-staged patients thereby selecting those patients for aggressive treatment and follow-up regimens. Moreover, the fact that *HOXA1* functionally drives metastatic phenotypes and tumor growth in addition to provide a prognostic gene signature also suggests that genes within this signature may represent individual gene targets or pathways, such as the TGF $\beta$  pathway,<sup>32</sup> suitable for therapeutic intervention.

## MATERIALS AND METHODS

### Cell culture

All cell lines were propagated at 37°C and 5% CO<sub>2</sub> in humidified atmosphere in RPMI-1640 medium (Invitrogen, Carlsbad, CA, USA) supplemented with 10% heat-inactivated fetal bovine serum (FBS). HMEL468 melanocytes were a subclone of PMEL/hTERT/CDK4(R24C)/p53DD/*BRAF*<sup>V600E</sup> cells, as described.<sup>13</sup> The WM115, WM278 and WM3211 cell lines were obtained from the Wistar Institute. The CHL-1 and SkMel30 cell lines were obtained from the ATCC (Manassas, VA, USA).

### Plasmids and RNAi

Full-length cDNA encoding *HOXA1* (NM\_005522.4) was obtained from the human ORFeome collection and transferred to the following viral vectors via Gateway recombination and virus production following manufacturer's recommendations: pLenti63/V5 DEST (Invitrogen), pInducer-20.<sup>33</sup> All overexpression studies were performed with newly transduced stable cell lines. For *SMAD3* knockdown, cells were transduced with virus generated from control and *pRetroSuper-SMAD3* (Addgene # 15726;<sup>34</sup>).

### Invasion assays

Matrigel-coated chambers (BD Biosciences, Franklin Lakes, NJ, USA; 354480) were utilized to assess invasiveness following manufacturer's suggestions and as described.<sup>10</sup> Chambers were seeded in triplicate or quadruplicate and placed in 10% serum-containing media which served as a chemo-attractant as well as in cell culture plates in duplicate as input controls. Following 20 h incubation, chambers were fixed in 10% formalin, stained with crystal violet for manual counting. Data were normalized to input cells to control for differences in cell number (loading control).



## Soft-agar and morphology assays

Soft-agar assays to measure anchorage-independent growth were performed as described.<sup>10</sup> For 3D Matrigel invasion morphology assays, cells transduced with control or *HOXA1* virus were resuspended in low density into 12% Matrigel at 800 cells/well.

## Animal

All studies using mice were performed in accordance with our IACUC-approved animal protocol at Baylor College of Medicine. For xenograft tumor assays, WM115 cells transduced with control or *HOXA1* lentivirus (in pLenti6.3-V5 and pInducer backbones) were stably selected and resuspended in a 1:1 solution of Hank's balanced salts (Invitrogen) and Matrigel (BD Bioscience) for subcutaneous implantation into female nude and NOD-SCID (for inducible studies) animals (Harlan, Indianapolis, IN, USA) at  $1.0 \times 10^6$  cells/site on both flanks. For the doxycycline induction experiment using pInducer-20-*HOXA1*, animals injected with transduced cells were separated into two cohorts and maintained with or without chow containing doxycycline (2 g/kg) for the duration of the experiment. For lung seeding assays, M3HRAS cells transduced with control of *HOXA1* virus were resuspended in Hank's balanced salts ( $1 \times 10^5$  cells in 200  $\mu$ l) for injection into the tail vein of female SCID (Harlan) mice followed by quantitation (lung/animal weight index) of lung tumor burden.

## Genomic and pathway analysis

The *HOXA1*-induced transcription analysis was conducted using RNAs extracted from WM115 cells transduced with either control or *HOXA1*, followed by hybridization of labeled cDNA onto Affymetrix (Santa Clara, CA, USA) GeneChips (Human Genome U133Plus2.0) by the Baylor College of Medicine Genome Profiling Core Facility (GEO# GSE37136). Data processing was carried out as described previously.<sup>18</sup> Two-sided homoscedastic *t*-tests (using log-transformed data) and fold changes were used to determine differentially expressed genes (for  $P < 0.01$  genes, False Discovery Rate estimated at 5%, using Storey method).<sup>35</sup> Functional Annotation Clustering (<http://david.abcc.ncifcrf.gov/>) and the IPA program were used to further analyze the cellular functions and pathways that were significantly regulated in the data set. To define the degree of *HOXA1* gene signature manifestation within profiles from an external data set, we used the previously described 't-score' metric.<sup>18</sup> Briefly, the *t*-score was defined for each external profile as the two-sided *t*-statistic comparing, within the profile, the average of the *HOXA1*-induced genes with the average of the *HOXA1*-repressed genes (genes within external data sets were first centered to standard deviations from the median; where multiple gene probes referred to the same gene, the probe with the highest variation was used).

## TGF $\beta$ assay

The TGF $\beta$  reporter assay was conducted using the p3TPLux reporter (Addgene #11767;<sup>17</sup>). WM115-*HOXA1* and control cells were seeded at  $2 \times 10^5$  cells per well in triplicate in 6-well plates 24 h before transfection with the p3TPLux reporter (1  $\mu$ g/well) and control reporter (Renilla, 20 ng/well). Following 24 h of incubation, cells were treated for 24 h with TGF $\beta$  (20 ng/ml, R&D Systems, Minneapolis, MN, USA) and were subjected to luciferase analysis (Promega, Madison, WI, USA) following manufacturer's protocol to assess reporter activation as indicated by the firefly/Renilla ratio. *P*-values were calculated using two-tailed *t*-test.

## Real-time qPCR

For analyses of gene expression, total RNA was isolated from cultured cells either expressing *HOXA1* or vector control. Coding regions were amplified by quantitative real-time PCR on a real-time PCR system, and the comparative cycle threshold method was used to quantify mRNA copy number. RNA expression levels were normalized to human Actin, and all validated PCR primer sets were purchased from SABiosciences (Qiagen, Valencia, CA, USA). TGF $\beta$ /BMP Signaling Pathway PCR Arrays (Qiagen) and analysis were performed according to manufacturer's recommendations.

## Immunoblot

Cells were washed twice in PBS and lysed using RIPA buffer containing 1 mM PMSF, 1  $\times$  Protease Inhibitor Cocktail (Sigma, St Louis, MO, USA) and 1  $\times$  Phosphatase inhibitor (Calbiochem, Billerica, MA, USA) for separation on 4–12% Bis-Tris gels (Bio-Rad, Hercules, CA, USA). The following

antibodies were used for immunoblotting following manufacturer's recommendations: MITF (Thermo); GAPDH (Santa Cruz, Santa Cruz, CA, USA); *HOXA1* (Sigma); Tubulin (Sigma).

## CONFLICT OF INTEREST

The authors declare no conflict of interest.

## ACKNOWLEDGEMENTS

KLS was supported by the American Cancer Society, and this work was supported by departmental seed funds to KLS from Baylor College of Medicine. This work was also supported by grants from the NIH (RO1 CA93947, U01 CA84313) to LC.

## REFERENCES

- Jemal A, Bray F, Center MM, Ferlay J, Ward E, Forman D. Global cancer statistics. *CA Cancer J Clin* 2011; **61**: 69–90.
- Valastyan S, Weinberg RA. Tumor metastasis: molecular insights and evolving paradigms. *Cell* 2011; **147**: 275–292.
- Bernards R, Weinberg RA. A progression puzzle. *Nature* 2002; **418**: 823.
- van de Vijver MJ, He YD, van't Veer LJ, Dai H, Hart AA, Voskuil DW et al. A gene-expression signature as a predictor of survival in breast cancer. *N Engl J Med* 2002; **347**: 1999–2009.
- Ding L, Ellis MJ, Li S, Larson DE, Chen K, Wallis JW et al. Genome remodelling in a basal-like breast cancer metastasis and xenograft. *Nature* 2010; **464**: 999–1005.
- Breslow A. Thickness, cross-sectional areas and depth of invasion in the prognosis of cutaneous melanoma. *Ann Surg* 1970; **172**: 902–908.
- Tuong W, Cheng LS, Armstrong AW. Melanoma: epidemiology, diagnosis, treatment, and outcomes. *Dermatol Clin* 2012; **30**: 113–124.
- Gimotty PA, Elder DE, Fraker DL, Botbyl J, Sellers K, Elenitsas R et al. Identification of high-risk patients among those diagnosed with thin cutaneous melanomas. *J Clin Oncol* 2007; **25**: 1129–1134.
- Criscione VD, Weinstock MA. Melanoma thickness trends in the United States, 1988–2006. *J Invest Dermatol* 2010; **130**: 793–797.
- Scott KL, Nogueira C, Heffernan TP, van Doorn R, Dhakal S, Hanna JA et al. Proinvasion metastasis drivers in early-stage melanoma are oncogenes. *Cancer Cell* 2011; **20**: 92–103.
- Chin L, Tam A, Pomerantz J, Wong M, Holash J, Bardeesy N et al. Essential role for oncogenic Ras in tumour maintenance. *Nature* 1999; **400**: 468–472.
- Kim M, Gans JD, Nogueira C, Wang A, Paik JH, Feng B et al. Comparative oncogenomics identifies NEDD9 as a melanoma metastasis gene. *Cell* 2006; **125**: 1269–1281.
- Garraway LA, Widlund HR, Rubin MA, Getz G, Berger AJ, Ramaswamy S et al. Integrative genomic analyses identify MITF as a lineage survival oncogene amplified in malignant melanoma. *Nature* 2005; **436**: 117–122.
- Remacle S, Shaw-Jackson C, Matis C, Lampe X, Picard J, Rezsoshy R. Changing homeodomain residues 2 and 3 of Hoxa1 alters its activity in a cell-type and enhancer dependent manner. *Nucleic Acids Res* 2002; **30**: 2663–2668.
- Svingen T, Tonissen KF. Hox transcription factors and their elusive mammalian gene targets. *Heredity* 2006; **97**: 88–96.
- Kaminska K, Wesolowska A, Danilkiewicz M. TGF beta signalling and its role in tumour pathogenesis. *Acta Biochim Pol* 2005; **52**: 329–337.
- Wrana JL, Attisano L, Carcamo J, Zentella A, Doody J, Laiho M et al. TGF beta signals through a heteromeric protein kinase receptor complex. *Cell* 1992; **71**: 1003–1014.
- Creighton CJ, Casa A, Lazard Z, Huang S, Tsimelzon A, Hilsenbeck SG et al. Insulin-like growth factor-I activates gene transcription programs strongly associated with poor breast cancer prognosis. *J Clin Oncol* 2008; **26**: 4078–4085.
- Hoek KS, Schlegel NC, Brafford P, Sucker A, Ugurel S, Kumar R et al. Metastatic potential of melanomas defined by specific gene expression profiles with no BRAF signature. *Pigment Cell Res* 2006; **19**: 290–302.
- Jeffs AR, Glover AC, Slobbe LJ, Wang L, He S, Hazlett JA et al. A gene expression signature of invasive potential in metastatic melanoma cells. *PLoS ONE* 2009; **4**: e8461.
- Timár J, Györfy B, Rásó E. Gene signature of the metastatic potential of cutaneous melanoma: too much for too little? *Clin Exp Metastasis* 2010; **27**: 371–387.
- Winnepenninckx V, Lazar V, Michiels S, Dessen P, Stas M, Alonso SR et al. Gene expression profiling of primary cutaneous melanoma and clinical outcome. *J Natl Cancer Inst* 2006; **98**: 472–482.
- Shah N, Sukumar S. The Hox genes and their roles in oncogenesis. *Nat Rev Cancer* 2010; **10**: 361–371.

- 24 Maeda K, Hamada J, Takahashi Y, Tada M, Yamamoto Y, Sugihara T *et al.* Altered expressions of HOX genes in human cutaneous malignant melanoma. *Int J Cancer* 2005; **114**: 436–441.
- 25 Gavalas A, Trainor P, Ariza-McNaughton L, Krumlauf R. Synergy between Hoxa1 and Hoxb1: the relationship between arch patterning and the generation of cranial neural crest. *Development* 2001; **128**: 3017–3027.
- 26 Carreira S, Goodall J, Denat L, Rodriguez M, Nuciforo P, Hoek KS *et al.* Mitf regulation of Dia1 controls melanoma proliferation and invasiveness. *Genes Dev* 2006; **20**: 3426–3439.
- 27 Lekmine F, Chang CK, Sethakorn N, Das Gupta TK, Salti GI. Role of microphthalmia transcription factor (Mitf) in melanoma differentiation. *Biochem Biophys Res Commun* 2007; **354**: 830–835.
- 28 Hoek KS, Goding CR. Cancer stem cells versus phenotype-switching in melanoma. *Pigment Cell Melanoma Res* 2010; **23**: 746–759.
- 29 Hoek KS, Eichhoff OM, Schlegel NC, Dobbeling U, Kobert N, Schaefer L *et al.* In vivo switching of human melanoma cells between proliferative and invasive states. *Cancer Res* 2008; **68**: 650–656.
- 30 Nishimura EK, Suzuki M, Igras V, Du J, Lonning S, Miyachi Y *et al.* Key roles for transforming growth factor  $\beta$  in melanocyte stem cell maintenance. *Stem Cell* 2010; **6**: 130–140.
- 31 Pinner S, Jordan P, Sharrock K, Bazley L, Collinson L, Marais R *et al.* Intravital imaging reveals transient changes in pigment production and Brn2 expression during metastatic melanoma dissemination. *Cancer Res* 2009; **69**: 7969–7977.
- 32 Mohammad KS, Javelaud D, Fournier PGJ, Niewolna M, McKenna CR, Peng XH *et al.* TGF- $\beta$ RI kinase inhibitor SD-208 reduces the development and progression of melanoma bone metastases. *Cancer Res* 2011; **71**: 175–184.
- 33 Meerbrey KL, Hu G, Kessler JD, Roarty K, Li MZ, Fang JE *et al.* The pINDUCER lentiviral toolkit for inducible RNA interference *in vitro* and *in vivo*. *Proc Natl Acad Sci USA* 2011; **108**: 3665–3670.
- 34 He W, Dorn DC, Erdjument-Bromage H, Tempst P, Moore MAS, Massagué J. Hematopoiesis controlled by distinct TIF1gamma and Smad4 branches of the TGFbeta pathway. *Cell* 2006; **125**: 929–941.
- 35 Storey JD, Tibshirani R. Statistical significance for genomewide studies. *Proc Natl Acad Sci USA* 2003; **100**: 9440–9445.

Supplementary Information accompanies the paper on the Oncogene website (<http://www.nature.com/onc>)